Biomolecule Arrays Using Functional Combinatorial Particle Patterning on Microchips

Felix Loeffler, Christopher Schirwitz, Jenny Wagner, Kai Koenig, Frieder Maerkle, Gloria Torralba, Michael Hausmann, F. Ralf Bischoff, Alexander Nesterov-Mueller, and Frank Breitling**

Biofunctionalization of surfaces in a microarray format has revolutionized biological assay applications. Here, a microarray system based on a microelectronic chip is presented that allows for a versatile combinatorial in situ molecule synthesis with very high density. Successfully demonstrating an application for peptide array synthesis, the method offers a compact approach, high combinatorial freedom, and, due to the intrinsic alignment, high and reproducible precision. Patterning the chip surface with different microparticle types which imbed different monomers, several thousand different molecule types can be simultaneously elongated layer-by-layer by coupling the particle imbedded monomers to the molecules growing on the chip surface. This technique has the potential for a wide application in combinatorial chemistry, as long as the desired monomeric building blocks are compatible with the chemical process.

1. Introduction

In the fields of genomics and transcriptomics, microarrays have revolutionized assay applications;[1,2] nevertheless, significant research effort is invested into technological improvements.[3,4] The fabrication of molecule libraries in a microarray format on solid surfaces allows for massively parallel high-throughput assays with frugal consumption of analyte; thus, it is one of the most important fields in biofunctionalization. Yet, it requires sophisticated technologies to facilitate such high-density arrays.

While the synthesis of DNA or RNA arrays only requires four different building blocks, highly versatile methods for combinatorial synthesis are required to generate peptides or polysaccharides.[5,6] In the case of natural peptides, 20 different building blocks (amino acid monomers) need to be processed in a fully combinatorial manner, yielding the possibility to assemble any desired peptide sequence.

Here, we describe the development and application of a microelectronic chip method which allows for the latter requirements in combinatorial in situ molecule synthesis. Recently, a proof of principle experiment has been described,[7] where two different peptides were synthesized in a chessboard pattern and therefore still lacking true combinatorics. Yet, it showed that this technique offers a spot density that approaches those of lithographic methods.[8] Lithographic synthesis methods, however, are based on liquids which entail several drawbacks regarding the amount of coupling cycle steps and the coupling yield. Hence, we immobilized activated monomers in solid particles, gaining several orders of magnitude in chemical stability compared to activated monomers in solvents.[7,9] Addressing the monomers by patterning the chip surface with different particle types, we can elongate several thousand different biomolecule types layer-by-layer simultaneously. We melt the particle matrix to initiate the monomer coupling, converting the particles into a gel-like phase, preserving the spatial pattern resolution. The integrity of these synthesized oligomers has been shown previously.[9]

The length of the in situ synthesized oligomer is only limited by the coupling yield, as in standard combinatorial chemistry. This technique has the potential for wide application in combinatorial chemistry, as long as the monomeric building blocks are compatible with the chemical steps. With low space requirements for the experimental setup, our method is easily extendable to up to 40 (e.g., D- and L- amino acids) or more monomeric building blocks, which allows for a high combinatorial freedom.

In the following, we apply our particle-based approach to fully combinatorial peptide array fabrication, enabling for the first time the parallel synthesis of 16 384 different peptides

F. Loeffler, C. Schirwitz, Dr. F. R. Bischoff
German Cancer Research Center
Chip-based Peptide Libraries Group
Im Neuenheimer Feld 580, 69120 Heidelberg, Germany
Dr. J. Wagner, Dr. K. Koenig, Dr. G. Torralba,
Prof. M. Hausmann
University of Heidelberg, Kirchhoff Institute for Physics
Peptide Chips Group, Im Neuenheimer Feld 227
69120 Heidelberg, Germany
F. Maerkle
Karlsruhe Institute of Technology,
Institute of Microstructure Technology
Hermann-von-Helmholtz-Platz 1
76344 Eggenstein-Leopoldshafen, Germany
Dr. A. Nesterov-Mueller, Dr. F. Breitling
Karlsruhe Institute of Technology
Institute of Microstructure Technology, Hermann-von-Helmholtz-Platz 1
76344 Eggenstein-Leopoldshafen, Germany
E-mail: alexander.nesterov-mueller@kit.edu; frank.breitling@kit.edu

DOI: 10.1002/adfm.201103103

(10 000 spots cm^{-2}) onto the surface of a microelectronic chip. Although arbitrary voltage patterns were achievable with microelectronic chips,[10] we observed that the contamination rate in any other pattern (other than the chessboard pattern consisting of only two different peptides) was still so high that combinatorial synthesis was practically impossible. Regarding this problem, we have theoretically and numerically analyzed particle dynamics,[11] leading to a crucial reduction of contamination by using new particles with very small diameters and an especially designed deposition device. Exploiting those improvements in on-chip particle deposition, we are now able to combinatorially deposit arbitrary particle patterns and different particle types with high precision and flexibility. We show that the consecutive deposition of 20 patterns with very low contamination is in fact possible. These advances have finally paved the way for a truly combinatorial application. In comparison to other particle patterning techniques,[12,13] our method offers a compact approach, a high combinatorial freedom, and, due to the intrinsic alignment, a comfortable pattern reproducibility.

In this article, we show the feasibility of our approach with a peptide array of synthesized HA- and FLAG-epitope variants and staining the array with different antibodies, demonstrating the influence of amino acid substitutions on antibody binding.[9,14]

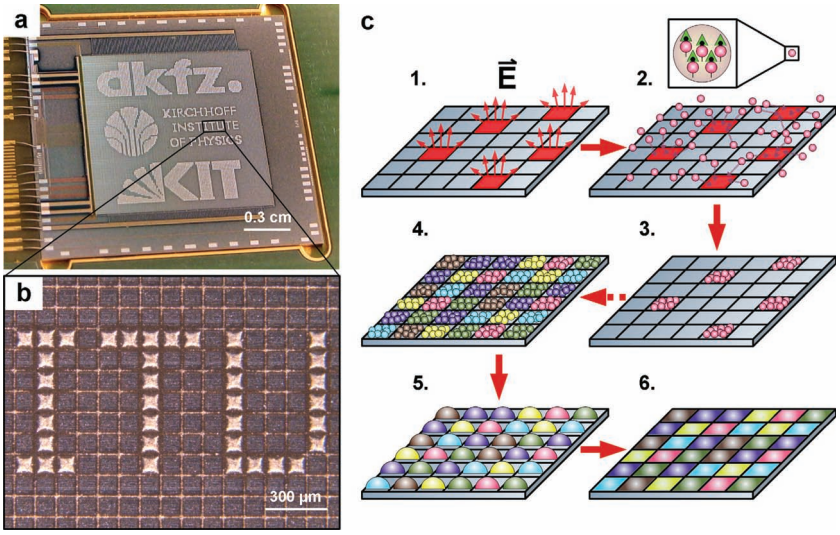

Figure 1. Microelectronic CMOS chip with deposition pattern. a) Chip, b) a magnified detail, and c) schematic deposition process: The chip is programmed to exhibit a voltage pattern on its surface (c1). Then, the chip is brought into contact with an aerosol of microparticles and the particles are attracted by the resulting electric field and are deposited according to the desired pattern (c2–3). The magnification of a particle (c2) shows that each particle type incorporates only one kind of monomeric building block (also see Figure 3). After application of a first particle type, the chip is reprogrammed to a different voltage pattern. Due to the high adhesion forces of the particles, the already deposited pattern remains on the surface without distortion. Next, the particle deposition is repeated with different particle types consecutively (c4), each type comprising a different monomer. These deposition steps can be repeated with hardly any cross reactions until the final deposition layer is completed. Afterwards, the chip is heated and, thus, the gel-like particle matrix releases the monomers for the coupling reaction to the surface (c5). Finally, the chip is subjected to several washing steps; the different monomers remain coupled to the pixels (c6). The complete process has to be repeated layer by layer until the terminal molecule length is reached (see Figure 3 for further information on the synthesis cycle).

2. New Materials and Methods

2.1. Chip and Basic Principle

The microelectronic CMOS (complementary metal oxide semiconductor) chip, shown in **Figure 1**a and b, features a total of 16 384 (128 × 128) pixel electrodes on its surface with a spot to spot pitch of 100 µm and a density of 10 000 pixels cm^{-2}. Higher spot densities of up to 40 000 pixels cm^{-2} are possible,[7,15] yet, for the sake of precision, quality, and robustness, we chose a lower spot density. The present chip is fabricated in a high-voltage CMOS process which allows for applying either 0 or up to 100 V to each pixel electrode in any desired pattern.

The chip surface is modified with a 40–50 nm thin copolymer film of poly(ethylene glycol) methacrylate (PEGMA) and methyl methacrylate (MMA) with mole fractions of 10% PEGMA and 90% MMA.[16,17] The coating provides for the functional hydroxyl groups which were subsequently modified with three β-alanine residues according to standard protocols to render the amino groups required for the synthesis.[18] Measurement of the starting density of amino groups upon Fmoc cleavage resulted in about 1 nmol cm^{-2} (also see the Supporting Information).

For combinatorial synthesis, the chip is programmed to exhibit a voltage pattern on its surface (Figure 1, c1). Then, the chip is exposed to an aerosol of microparticles (**Figure 2**): Particles are only attracted and deposited onto those pixel electrodes which exhibit an electric field. The voltage pattern is thus, transformed into the according particle pattern with high precision (Figure 1, c2–3).[11] A key feature in this process is that particles will only reach the chip surface, where the local electric field of a switched on electrode attracts particles. Once particles have contact with the surface, adhesion forces become so dominant that particles stick to the surface and conserve the deposition pattern. The magnification of a single particle (Figure 1, c2) illustrates that each particle type incorporates only one kind of monomeric building block. After application of a first particle type, the chip is reprogrammed to a different voltage pattern. Due to the high adhesion forces of the particles, the already deposited pattern remains on the surface without distortion. Next, we repeat the particle deposition consecutively without overlap of the different particle types (Figure 1, c4), each type comprising a different monomer. These deposition steps can be repeated with hardly any wrongly deposited particles until the final deposition layer is completed (see the Supporting Information). Afterwards, the chip is heated and the particle matrix melts and forms distinct gel-like reaction spheres. Similar to Merrifield's solid-phase peptide synthesis,[19] the particle

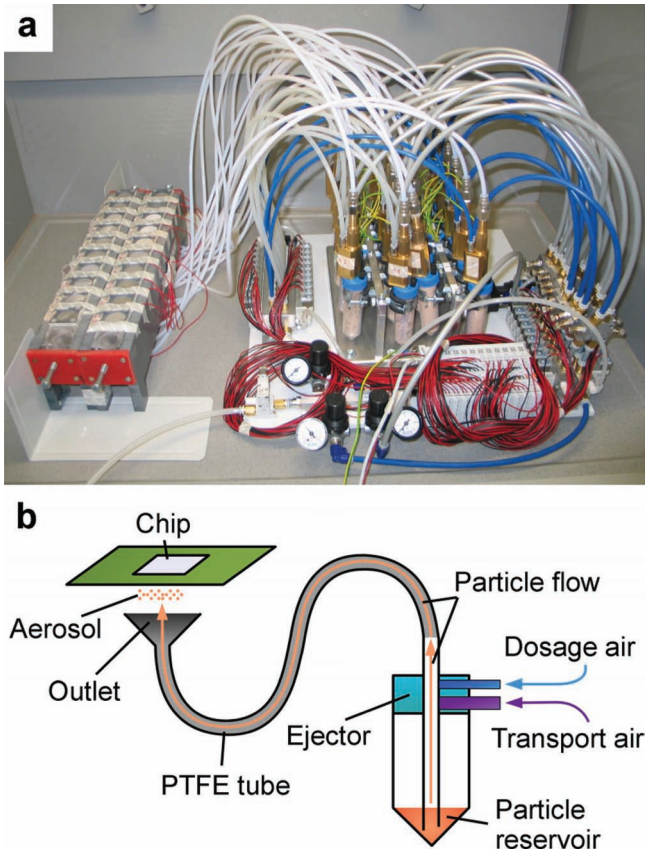

Figure 2. Aerosol generator for 20 different particle types. a) Aerosol generator and b) schematic of aerosol generation and deposition principle for one particle type: particles are siphoned out of a particle reservoir using the air ejector principle, two different air inlets (dosage and transport air) not only provide for the desired siphoning effect, but can also be used to control the aerosol density and velocity (for further details, see text)

matrix releases the monomers, which now couple to the surface bound amino groups, without losing the spatial resolution of the deposition pattern (Figure 1, c5). Then, the chip is allowed to cool to room temperature, which causes the reaction spheres to solidify, freezing the coupling reaction. Finally, the chip is subjected to several washing steps, removing excess monomers and the particle matrix. Yet, the different monomers remain coupled to the pixel surface (Figure 1, c6). The complete process cycle is repeated layer by layer until the terminal molecule length is reached (see **Figure 3** for further information on the coupling and synthesis cycle).

2.2. Aerosol Generation and Deposition

To generate an aerosol for particle deposition, we have designed a computer controlled aerosol generator (in cooperation with R.O.T GmbH[20]) to ensure reproducible aerosol properties (Figure 2a). It allows us to generate 20 different aerosol types, corresponding to the 20 proteinogenic amino acids. The process of aerosol generation is shown in Figure 2b: particles are siphoned out of a particle reservoir using the air ejector principle. Two different air inlets (dosage and transport air) not only provide for the desired siphoning effect, but can also be used to control the aerosol density and velocity.

The particles are ejected through a polytetrafluoroethylene (PTFE) tube which leads to triboelectric particle charging. Afterwards, they are brought into contact with the chip at an outlet with an especially designed geometry (Figure S1 in the Supporting Information). A negatively charged sieve filters and selects the particle size and particle charge to ensure a high precision of the deposition pattern.[11] The surface-to-volume ratio of the particles is large due to the rather small size of the particles (about 4 µm in diameter). Therefore, minor surface friction suffices for the charging. Hence, it is unnecessary to implement an additional special setup for further triboelectric particle charging.

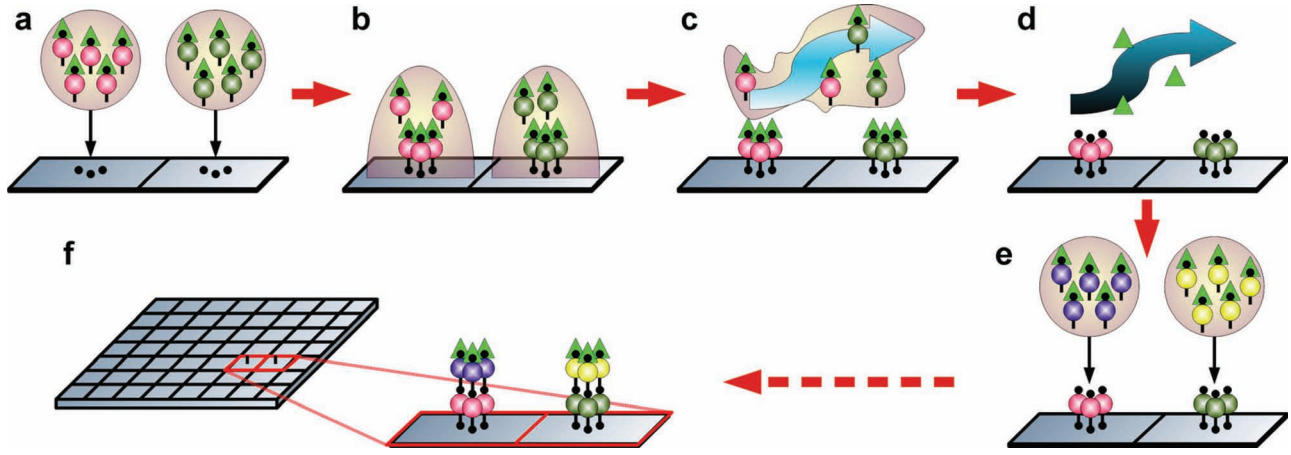

Figure 3. Combinatorial synthesis of a (peptide) molecule array. a) First, the particles are transferred to a substrate. Each particle type contains a different (amino acid) building block, represented as colored spheres. b) Afterwards, the particles are melted and the monomeric building blocks couple to the surface. c) Then, the melted matrix and uncoupled monomers are washed away and finally, d) the protective groups (green triangles) are removed. e,f) These steps are repeated with different particle patterns until the desired array is completed.

We used an aerosol generator consisting of 20 different reservoirs and outlets to deposit the different particle types, each containing a different amino acid monomer, consecutively onto the chip.

2.3. Particles and Synthesis

The particles,[9] used in the process, are composed of 84.5% w/w polymer matrix, 10% w/w of Fmoc (9-fluorenylmethoxycarbonyl)-protected amino acid monomer pre-activated as OPfp (pentafluorophenyl) ester, 4.5% w/w pyrazolone orange, and 1.0% w/w of Fe(naphthol)$_2$ complex,[21] acting as a charge control agent. The compound is homogenized and afterwards air milled. Finally, 0.05% w/w silica nanoparticles are added to improve flow properties and to prevent agglomeration.

We produced twenty different particle types, each containing a different amino acid monomer. The obtained mean charge per mass ratio of the different particle types was about -3 mC kg^{-1}.[11]

The combinatorial synthesis of an array is shown in Figure 3. First, particles are deposited onto the functionalized substrate exhibiting the reactive amino groups (black dots; Figure 3a). Each particle type imbeds a different amino acid type, as illustrated by the differently colored spheres. When the particle matrix (in gray) is melted, the OPfp preactivated amino acids diffuse and couple to the amino groups on the surface (Figure 3b). Afterwards, excess particles (gray matrix) and uncoupled monomers are washed away (Figure 3c), using a mixture of dimethylformamide, acetic anhydride, and diisopropylethylamine (DMF/Ac_2O/DIPEA) which at the same time acetylates (i.e., caps) unreacted amino groups. Finally, the Fmoc-protecting groups (green triangles) are removed from the coupled monomers (Figure 3d), using a solution of 20% piperidine in DMF. Hence, new amino groups are presented on the surface for the next coupling cycle. This procedure is repeated with layers of different particle patterns (Figure 3e and f), until the desired combinatorial array is completed. In the end, side-chain protecting groups are cleaved with trifluoroacetic acid (TFA) (for more details, see the Supporting information).

Using this technique, it is easily possible to generate a variety of biologically or chemically different molecules, given that the building blocks are compatible with the synthesis reaction. The maximum achievable peptide length depends on the amino acid coupling yield, which is about 90%.[9] Since the signal-to-noise ratio (peptides to truncated peptides) might become increasingly relevant, we require a total peptide yield of at least 10%. Thus, in our case, the maximum peptide length is about 20 amino acids with a density of 0.1 nmol cm$^{-2;}$ the rest of the peptides are truncated.

2.4. Fluorescent Staining and Antibodies

The peptide arrays were blocked in blocking buffer for fluorescent western blotting (Rockland Immunochemicals, Inc.). Afterwards, the arrays were incubated with monoclonal mouse anti-HA IgG antibodies and polyclonal rabbit anti-FLAG IgG antibodies, diluted (1:500) in phosphate buffer saline (PBS) with 1:10 blocking buffer and supplemented with 0.05% v/v polysorbate 20 (PS20). The binding was detected with the corresponding secondary antibodies goat anti-mouse conjugated with the fluorescent dye Alexa Fluor 546 and goat anti-rabbit conjugated with Alexa Fluor 647 (diluted 1:1000 in: PBS + PS20 + 1:10 blocking buffer). Monoclonal antibodies are generally derived from one B-cell clone and are identical and monospecific. Polyclonal antibodies are a mixture of antibodies, all directed against one antigen, but non-monospecific.

2.5. Fluorescent Image Acquisition

The fluorescent images were obtained with a Molecular Devices GenePix 4000B microarray scanner. The shown images were only adjusted in brightness and contrast.

3. Results and Discussion

Proving the concept, we synthesized an array with 1536 different variants of the 9meric FLAG-epitope (N-Tyr-Asp-Tyr-Lys-Asp-Asp-Asp-Asp-Lys-C) and the 9meric HA-epitope (N-Tyr-Pro-Tyr-Asp- Val-Pro-Asp-Tyr-Ala-C). We altered the epitopes and replaced different amino acids to investigate their importance in specific antibody binding (**Figure 4**a and b). All synthesized variants of the HA-epitope are listed in **Table 1**. The array is framed by an alternation of HA-, FLAG-, and another control peptide (N-Asp-Ala-Asp-Asp-Pro-Asp-Asp-Ala-C). We incubated the array with monoclonal mouse anti-HA IgG antibodies and polyclonal rabbit anti-FLAG IgG antibodies. Bound antibodies were detected with corresponding secondary antibodies conjugated with the fluorescent dyes Alexa Fluor 546 and Alexa Fluor 647, respectively.

In Figure 4a, the green channel shows the fluorescence pattern of the monoclonal anti-HA antibody. Several control spots are visible in a regular diagonal pattern and only a few HA-epitope variants, highlighted with red rectangles, were intensively stained by the monoclonal antibody, indicating good binding. Table 1 shows the influence of amino acid substitutions in the HA-epitope on binding of the monoclonal mouse anti-HA antibody.

With this limited number of peptide variants and, therefore, a rather subjective approach, together with other experiments (Figure S2 in the Supporting Information), we can derive a sequence which seems to offer a similar binding efficiency as the wild type HA-epitope. The three most important amino acids in binding of the monoclonal Anti-HA antibody are Asp in position 4 and 7 and Ala in position 9. However, peptides containing an acidic residue (Asp) in the positions 5, 6, or 8 showed no measurable binding signal (see Table 1). In this instance we could rule out the possibility of insufficient synthesis or peptide quality, since four adjacent Asp residues were successfully synthesized and stained in the FLAG-epitope.

Comparing the fluorescence intensities of four different peptide spots in Figure 4* and ** (the standard HA-epitope and three variants), the influence of amino acid substitutions, highlighted with red rectangles in the peptide sequence, on the binding of the monoclonal mouse anti-HA antibody is

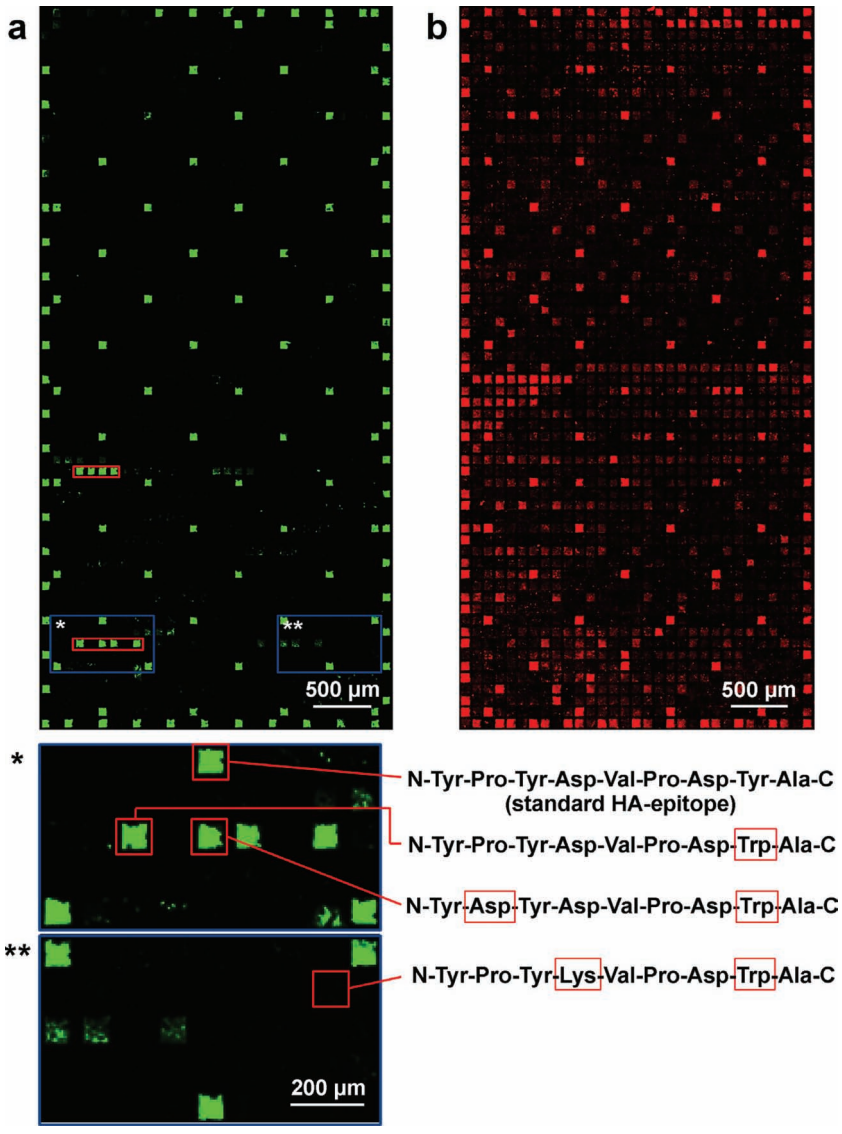

Figure 4. Peptide array of 31 × 65. Also see Table 1 and 2. The array was incubated with monoclonal mouse anti-HA IgG antibodies and polyclonal rabbit anti-FLAG IgG antibodies and stained with the two secondary IgG antibodies goat anti-mouse conjugated with a) Alexa Fluor 546 and b) goat anti-rabbit conjugated with Alexa Fluor 647. The array is framed by an alternation of HA-, FLAG-, and another control peptide (see text). In (a) good binders of the monoclonal mouse anti-HA antibody to altered HA-epitopes are highlighted with red rectangles. Panels (*) and (**) show magnified details of the array in (a): the fluorescence intensities of four different peptide spots (the standard HA-epitope and three variants) demonstrate the influence of amino acid substitutions (highlighted with red rectangles in the sequence) on the binding of the monoclonal mouse anti-HA antibody. In (b), the red channel shows various binders with distinct binding efficiencies for the polyclonal rabbit anti-FLAG antibody.

demonstrated. The standard HA-epitope (upper spot) shows, as expected, a bright staining, whereas the left central peptide spot with only one substitution in the 8th position (Trp instead of Tyr) and the central spot with the latter substitution together with Asp instead of Pro in the 2nd position still preserve a good binding to the monoclonal antibody. The right spot in Figure 4** with the sequence N-Tyr-Pro-Tyr-Lys-Val-Pro-Asp-Trp-Ala-C shows no binding. This indicates the importance of the acidic Asp residue in position 4, because a substitution with a basic Lys completely prohibits binding. Repeated experiments showed reproducibly the same results, which prove the robustness of the system.

In Figure 4b, the red channel shows the staining result using a polyclonal Anti-FLAG antibody. The FLAG variants are listed in **Table 2**. As expected, and in contrast to the monoclonal HA antibody, the polyclonal serum shows more promiscuous binding towards epitope variants. We could identify a preference for poly-Asp, especially four and five (more or less) adjacent Asp residues, resembling the C-terminus of the FLAG-epitope. On the other hand, we could observe strong binding of peptides with the amino acid sequence N-Tyr-Asp-Tyr-Lys-Asp-Asp- *Xxx-Xxx-Xxx*-C, which corresponds to the five N-terminal amino acids of the FLAG-epitope. Additionally, some species of the polyclonal antibodies seem to bind weakly to the control peptide N-Asp-Ala-Asp-Asp-Pro-Asp-Asp-Ala-C, which is located in the array frame, being a repeated alternation of HA- (bright red), FLAG- (bright green), and control epitope (light red).

Some peptide spots exhibit background noise in fluorescent imaging and we also observed a slight intensity fluctuation over the array surface. This may be due to the sometimes insufficient particle pattern quality, the inhomogenous surface coating and the staining process which so far has to be done manually with all typical shortcomings in preparing microtechniques by hand. Additionally, our in situ technique does not yet allow for a purification of the synthesized peptides and, as the drawbacks in sequence-dependent yield of solid phase peptide chemistry are well known, the practical yield has an increasing impact on fluorescence intensity with increasing peptide length. Thus, enhancing the coupling yield of amino acids (e.g., pre-swelling of copolymer with DMF) will be a future objective. Further improvements of the peptide microchip will therefore, on the one hand, mainly comprise the optimization of surface coating and particle quality reproducibility, which are the critical players in biofunctional high-precision particle deposition. On the other hand, future developments should be also devised in the scope of automation: robotics, used in particle deposition, chip handling, and "wet" chemical coupling steps will improve the robustness of the procedure for routine applications. The complete process will be associated with automatic quality control as already described for the particle pattern.[22] Successful tackling of all these process steps will finally allow for an automated routine application of this research tool.

Table 1. Influence of amino acid substitutions on the binding of the monoclonal mouse anti-HA antibody to an altered HA-epitope.

Amino acid #		1	2	3	4	5	6	7	8	9	
HA-epitope	N-	Tyr	Pro	Tyr	Asp	Val	Pro	Asp	Tyr	Ala	-C
Good binding			Asp	Ala					Trp		
Poor or no binding					Glu/ Lys	Asp	Asp	Glu/ Asn/ Gln	Asp/ Asn	Lys	

Table 2. Amino acid substitutions in the FLAG-epitope facilitated for the binding assay of the polyclonal rabbit-Anti-FLAG antibodies (1536 different variants)

FLAG-epitope	N-	Tyr	Asp	Tyr	Lys	Asp	Asp	Asp	Asp	Lys	-C
Possible amino acid variants			Pro	Ala	Glu/ Asp	Val	Pro	Glu/ Asn/ Gln	Trp/ Asn/ Tyr	Ala	

This fully combinatorial peptide array facilitated on a microelectronic chip using microparticle patterning shows the feasibility of our approach. The method presented here offers an unprecedented spot density for in situ combinatorial arrays; the coupling yield is comparable to standard combinatorial chemistry. Furthermore, the method is easily extendable to D-amino acids, which makes it applicable in synthetic peptide drug discovery. We propose that this method is applicable not only in the medical and biological fields of peptide synthesis, but also has the potential for a wide application in general combinatorial approaches, e.g., peptidomimetics, which can be used in chemical screenings for catalysts or for new organic electronics. Today's CMOS technique is mature and advanced, providing cost-efficient microchips and, thus, making this process feasible for biomolecule array production. By means of further miniaturization, the spot count and density can be easily increased.[15]

Supporting Information

Supporting Information is available from the Wiley Online Library or from the author.

Acknowledgements

The authors thank J. Kretschmer, D. Rambow, and R. Achenbach for technical assistance. The financial support of the Baden-Württemberg Stiftung is gratefully acknowledged.

Received: December 21, 2011
Published online: April 5, 2012

[1] P. A. Carr, G. M. Church, *Nat. Biotechnol.* **2009**, *27*, 1151.
[2] J. D. Hoheisel, *Nat. Rev. Genet.* **2006**, *7*, 200.
[3] J. D. Tian, J. Y. Quan, I. Saaem, N. Tang, S. M. Ma, N. Negre, H. Gong, K. P. White, *Nat. Biotechnol.* **2011**, *29*, 449.
[4] S. Kosuri, N. Eroshenko, E. M. LeProust, M. Super, J. Way, J. B. Li, G. M. Church, *Nat. Biotechnol.* **2010**, *28*, 1295.
[5] M. Uttamchandani, S. Q. Yao, *Curr. Pharm. Design* **2008**, *14*, 2428.
[6] L. Cipolla, F. Peri, B. La Ferla, C. Redaelli, F. Nicotra, *Curr. Org. Synth.* **2005**, *2*, 153.
[7] M. Beyer, A. Nesterov, I. Block, K. Konig, T. Felgenhauer, S. Fernandez, K. Leibe, G. Torralba, M. Hausmann, U. Trunk, V. Lindenstruth, F. R. Bischoff, V. Stadler, F. Breitling, *Science* **2007**, *318*, 1888.
[8] S. P. A. Fodor, J. L. Read, M. C. Pirrung, L. Stryer, A. T. Lu, D. Solas, *Science* **1991**, *251*, 767.
[9] V. Stadler, T. Felgenhauer, M. Beyer, S. Fernandez, K. Leibe, S. Guttler, M. Groning, K. Konig, G. Torralba, M. Hausmann, V. Lindenstruth, A. Nesterov, I. Block, R. Pipkorn, A. Poustka, F. R. Bischoff, F. Breitling, *Angew. Chem., Int. Ed.* **2008**, *47*, 7132.
[10] K. Koenig, I. Block, A. Nesterov, G. Torralba, S. Fernandez, T. Felgenhauer, K. Leibe, C. Schirwitz, F. Loeffler, F. Painke, J. Wagner, U. Trunk, F. R. Bischoff, F. Breitling, V. Stadler, M. Hausmann, V. Lindenstruth, *Sens. Actuators, B* **2010**, *147*, 418.
[11] F. Loeffler, J. Wagner, K. Koenig, F. Maerkle, S. Fernandez, C. Schirwitz, G. Torralba, M. Hausmann, V. Lindenstruth, F. R. Bischoff, F. Breitling, A. Nesterov, *Aerosol Sci. Technol.* **2011**, *45*, 65.
[12] H. O. Jacobs, G. M. Whitesides, *Science* **2001**, *291*, 1763–1766.
[13] N. R. Bieri, J. Chung, S. E. Haferl, D. Poulikakos, C. P. Grigoropoulos, *Appl. Phys. Lett.* **2003**, *82*, 3529.
[14] G. J. Wegner, H. J. Lee, R. M. Corn, *Anal. Chem.* **2002**, *74*, 5161.
[15] J. Wagner, K. Koenig, T. Förtsch, F. Loeffler, S. Fernandez, T. Felgenhauer, C. Schirwitz, F. Painke, G. Torralba, V. Lindenstruth, F. R. Bischoff, V. Stadler, F. Breitling, M. Hausmann, A. Nesterov-Müller, *Sens. Actuators, A* **2011**, *172*, 533.
[16] M. Beyer, T. Felgenhauer, F. R. Bischoff, F. Breitling, *Biomaterials* **2006**, *27*, 3505.
[17] V. Stadler, R. Kirmse, M. Beyer, F. Breitling, T. Ludwig, F. R. Bischoff, *Langmuir* **2008**, *24*, 8151.
[18] A. Nesterov, E. Dörsam, Y.-C. Cheng, C. Schirwitz, F. Märkle, F. Löffler, K. König, V. Stadler, F. R. Bischoff, F. Breitling, in *Small Molecule Microarrays: Methods and Protocols*, Eds.: M. Uttamchandani, S.Q.Q. Yao, Springer Protocols, **2010**, pp. 109–124.
[19] R. B. Merrifield, *Science* **1965**, *150*, 178.
[20] Hompage of ROT company, http://www.r-o-t-gmbh.de/, (accessed March 2012).
[21] Y. Kawagishi, Y. Ishida, K. Ishikawa, (Orient Chemical Industries, Ltd. (JP)), *US 4404271* **1983**.
[22] J. Wagner, F. Loffler, K. Konig, S. Fernandez, A. Nesterov-Muller, F. Breitling, F. R. Bischoff, V. Stadler, M. Hausmann, V. Lindenstruth, *Rev. Sci. Instrum.* **2010**, *81*, 073703.